J Electroceram (2012) 29:12–22
DOI 10.1007/s10832-012-9731-6

Optical and photoluminescence properties of Ga doped ZnO nanostructures by sol-gel method

D.-T. Phan · A. A. M. Farag · F. Yakuphanoglu · G. S. Chung

Received: 24 December 2011 / Accepted: 16 April 2012 / Published online: 11 May 2012

Abstract Zinc oxide (ZnO) nanocrystallites with different Ga-doping levels were successfully prepared by spin coating sol–gel technique. The morphological properties of Ga doped ZnO films were studied by atomic force microscopy (AFM). Alignment of ZnO nanorods with respect to the substrate depends on the amount of Ga dopant content. The dopant content varies from 1 % to 4 %, based on Ga-doping levels. The optical properties of the ZnO nanocrystallites following Ga-doping were also investigated by UV–Visible absorption and Photoluminescence spectra. Our results indicate that Ga-doping can change the energy-band structure and effectively adjust the intensity of the luminescence properties of ZnO nanocrystallites. Transmittance spectra of the films indicate that the films have high transparency. The refractive index dispersion was analyzed by single oscillator model developed by Wemple and DiDomenico. The oscillator energy, dispersion energy, high frequency dielectric constant values for the films were determined were calculated and it is found that the optical parameters are changed with Ga-doping content.

Keywords Ga-doped ZnO · Photoluminscence · nanorods · Optical dispersion

D.-T. Phan · G. S. Chung
School of Electrical Engineering, University of Ulsan,
San 29, Mugeodong, Namgu,
Ulsan 680-749, South Korea

G. S. Chung
e-mail: gschung@ulsan.ac.kr

A. A. M. Farag
Thin Film Laboratory, Physics Department, Faculty of Education,
Ain Shams University,
Cairo 11757, Egypt

F. Yakuphanoglu (✉)
Physics Department, Faculty of Science, Firat University,
23119 Elazig, Turkey
e-mail: fyhanoglu@firat.edu.tr

F. Yakuphanoglu
e-mail: fyhan@hotmail.com

1 Introduction

Nanostructured ZnO-based materials possess unique position among materials owing to its superior and diverse properties such as piezoelectricity, chemical stability, biocompatibility, optical transparency in the visible region, high voltage current nonlinearity and widely used for applications such as photoconductors, logic gate and field emitters [1, 2]. Recently, applications of ZnO nanorods and thin films in energy conversion, such as in electronic and optoelectronic devices such as transparent conductors, solar cell windows, gas sensors, surface acoustic wave (SAW) devices, heat mirrors, dye sensitized solar cells and thermoelectronics, have attracted increasing research interest [1–5].

The addition of selective doping element such as B, Al, Ga, In,Ni and Co into ZnO has become an important route for enhancing and controlling its optical, electrical performance, which are crucial for their practical applications [6, 7].

The physical properties of undoped and doped ZnO films have been widely reported. Vijayalakshmi et al. [8] studied the effect of Cd dopant on the properties of ZnO films. Shan et al. [9] deposited undoped ZnO, and Mg and Cd-doped ZnO thin films using pulsed laser deposition (PLD) and investigated their structural, morphological and optical properties.

Effect of In, Al and Sn dopants on the optical and structural properties of ZnO thin films have been investigated by Caglar et al. [10]. Ilican et al. [11] studied the structural, optical and electrical properties of the Sb-doped ZnO films by various

techniques including scanning electron microscopy, X-ray diffraction, UV–vis absorption, photoluminescence, and electrical transport measurements. The microstructure, and the electrical and optical properties of undoped zinc oxide (ZnO) and cadmium-doped ZnO (CZO) films deposited by a sol–gel method have been investigated by Yakuphanoglu et al. [12]. The effect of Ni contents on the structural, photoluminescence (PL) and Optical constants properties of undoped and Ni-doped ZnO of 0.2 %, 0.4 %, 0.6 %, 0.8 %, 1 %, 3 %, 5 % and 7 % concentrations were investigated by Farag et al. [13]. Moreover, the effect of Cu incorporation on the structural, morphological and optical properties of the ZnO film was investigated by Caglar and Yakuphanoglu [14].

Among these metal dopants, the Ga doping seems to be promising due to its advantages, such as the rather similar ionic radius and the covalent radius (0.062 and 0.126 nm), as compared to those of Zn (0.074 and 0.134 nm), respectively [15, 16]. Therefore, the Ga^{3+} can be substituted for Zn^{2+} without any lattice distortion and can cause free-stress in film [15, 16]. Moreover, the Ga-doped ZnO thin films have a larger optical transmittance and smaller resistance than In- and Al-doped ZnO films, which are very important for perfect transparent conducting oxides [16, 17].

Although several experimental studies have been reported on the structural, morphological, and optical properties of doped ZnO films, there are few reports on the optical constants of Ga-doped ZnO in the available literature. The objective of the present work is to prepare undoped and Ga-doped ZnO nanostructure films by using simple sol gel spin coating method with controlling Ga contents. The photoluminescence, PL is also studied for providing information on the quality of surfaces and interfaces. The main important optical parameters such as refractive index, absorption index, absorption coefficient, optical band gap, real and imaginary parts of dielectric constant and optical conductivity, the high frequency dielectric constant and the lattice dielectric constant and single oscillator parameters are calculated and interpreted for the undoped and Ga-doped ZnO films.

2 Experimental

2.1 Materials, preparation and characterization tools

ZnO and Ga-doped nanostructured films were prepared by sol–gel method using spin coating technique onto ITO coated conducting glass substrates. These substrates were cleaned by chemical method using ultrasonic cleaner and dried with nitrogen. The Ga doped-ZnO coating solutions were prepared from zinc acetate dihydrate ($ZnO(CH_3COO)_2 \cdot 2H_2O$, Sigma-aldrich), Gallium(III) nitrate hydrate ($Ga(NO_3) \cdot H_2O$, Alfa Aesar), methoxyethanol, and monoethanolamine (Samchun pure chemical) and the solution were stirred for 2 h at 70°C using a hot plate magnetic stirrer. The obtained solutions were aged at room temperature for 3 days to evaporate all the solvent and to remove all the organic residuals. The Ga dopant level, determined by $100\times[m_{Ga}]/[m_{Ga}+m_{ZnO}]$, was varied from 0 to 4 wt.%, where m_x is the mass of component x. Then, the Ga-doped ZnO layers were coated on the cleaned glass by spin coater at room temperature with 1000–2500 rpm. The films were thermally treated at 300° C for 10 min. using a hotplate. The coatings were repeated for eight times to obtain a ZnO film of approximately 240 nm thickness. The thickness of the films was determined with Mettler Toledo MX5 microbalance using weighing method for all the deposited films. The prepared film structures were found to be nearly similar to wt% of Ga in solution.

The surface morphology of the prepared films was observed by atomic force microscopy, AFM (type Park System XE-100E).

The photoluminescence properties of the films were recorded using a fluorescence spectrophotometer (LS 45) with an excitation wavelength of 325 nm. The measurements of transmittance $T(\lambda)$ and reflectance $R(\lambda)$ were carried out using a Shimadzu UV–VIS-NIR 3600 spectrophotometer with an integrating sphere attachment. All the measurements were carried out at room temperature.

2.2 Method of optical constants calculations

For determination of the optical constants of the films, undoped ZnO and Ga doped ZnO thin films were deposited onto glass transparent substrates. The complex refractive index for the films is expressed by $\widetilde{n} = n - ik$, where n is the refractive index and k is the extinction coefficient. The absorption coefficient α was computed from the experimental measurements of the transmittance $T(\lambda)$ and reflectance $R(\lambda)$ using the following equation [18]:

$$\alpha = \frac{1}{d}\ln\left[\frac{(1-R^2)}{2T} + \sqrt{\frac{(1-R)^4}{4T^2} + R^2}\right] \quad (1)$$

The reflectance $R(\lambda)$ can be expressed by Fresnel formula [19]:

$$R = \frac{(n-1)^2 + k^2}{(n+1)^2 + k^2} \quad (2)$$

Where $k=\alpha\lambda/4\pi$. If one solves Eq. (2) via elementary algebraic manipulation, the refractive index is obtained as

$$n = \left(\frac{1+R}{1-R}\right) + \sqrt{\frac{4R}{(1-R)^2} - k^2} \quad (3)$$

When the film thickness is known, then the computation can be carried out and the optical constants can be

calculated. The optical constants n and k were estimated by taking the consideration of the experimental errors in measuring the film thickness as ±2 %, and $T(\lambda)$and $R(\lambda)$ as ±1 %.

3 Results and discussion

3.1 Surface morphological characterizations

Figure 1 shows AFM images of the ZnO and Ga-doped ZnO films. ZnO has a high nucleation density and forms continuous thin films without nanorods-shaped grains as well as the films of low Ga concentrations of 1 % and 2 %. On the other hand, the images of higher Ga concentrations of 3 % and 4 % indicate that these films are formed from the nanorods of different alignments and the alignment was enhanced with increasing Ga content in ZnO. The incorporation of Ga dopants promoted the formation of vertically arrayed nanorods by inducing island growth in the initial stage. As the Ga contents increased, the density of the stacking faults formed by stress relaxation process was greatly enhanced [20]. However, the incorporation of the Ga dopants of 3 % and 4 % forms a high density of stacking of the nanorods. Notably, the stacking fault density was significantly enhanced by the increase in the Ga content, which is considered to be attributed to the structural relaxation of the stored stress [20]. The metal doping is the effective procedure to modify the grain size, orientation and the conductivity and could greatly influence the crystalline, optical and the electrical properties of the ZnO nanostructures [21]. For many nanorod applications, such as field emission, it is important to control alignment of nanorods [22].

3.2 Photoluminescence and absorption characterization

It is well known that the intensity of the photoluminescence, PL signal provides information on the quality of surfaces and interfaces. Generally, the PL of ZnO films exhibits one emission peak in the UV region due to a recombination of free excitons, and possibly one or more emission peaks in the visible spectral range, which are attributed to defect emissions [23]. However, the origin of the defects responsible for these emissions is not fully clear but still there are lots of controversial explanations for these emissions in ZnO nanoparticles [23]. Generally, the near band emission in ZnO is observed around 400 nm may be attributed to the oxygen-deficient non-stoichiometric nature of the materials [24]. Figure 2 shows PL spectra of the ZnO and different Ga-doped ZnO films. A nearly similar feature of the obtained PL spectra with inhancement in the intensity was observed for the Ga-doped ZnO as compared to ZnO spectrum. This enhancement for the PL spectra due to the incorporation of Ga dopant in the ZnO host material may be attributed to the surface states and enhance the number of defects in the material as discussed by Wang et al. [25] for Co-doping in ZnO namostructured films. Therefore, the possible strong visible emissions in Ga-doping in ZnO nanocrystals may arise due to the electronic transitions from the deep levels, surface states levels to conduction band.

The emission observed around 440 nm (2.82 eV) may be attributed to the exciton recombination between the electron localized at the interstitial zinc and the holes in the valence band [23, 26]. The weak emission observed around 475 nm may result from the electron transition from the level of the ionized oxygen vacancies to the valence band [27]. The emission observed at 540 nm (2.29 eV) is attributed to the radiative recombination of delocalized electrons close to the conduction band with deeply trapped holes in oxygen centers [23, 28].

Figure 3 shows the absorption of corresponding UV–visible spectra of undoped and Ga-doped ZnO nanostructured thin films. The intensity of the absorption spectra in the higher energy region increases from the undoped ZnO to 2 % Ga doped ZnO after which the intensity decreases. Otherwise, a regular change in the absorption spectra is observed in the low energy region where the intensity increases from the undoped ZnO to 4 % Ga doped ZnO films. The sharp edge of the absorption spectrum of 4 % Ga-doped ZnO film as compared to the other films may be attributed to the well ordered and condensed distribution of the nanorods for the 4 % Ga-doped ZnO film as compared to the other films as supported before by using AFM images.

3.3 Optical constant characterization

The spectral behavior of the normal incidence transmittance $T(\lambda)$ and reflectance $R(\lambda)$ for the ZnO and Ga-doped ZnO nanostructure thin films are shown in Fig. 4 (a) and (b). As seen in Fig. 4(a), the observed high transmitivity of these films suggests that all films have a good transparency, especially above 500 nm wavelength. A sharp decrease in the transmittance is observed at about 370 nm that is attributed to the band edge absorption. This strong absorption means that the incoming photons have sufficient energy to excite electrons from the valence band to the conduction band. Also, a little dependence is observed for the measured transmittance on the doping concentration of Ga at the studied range especially near the band edge. The spectral behavior of the reflectance $R(\lambda)$ in Fig. 4(b) shows a doping concentration of Ga dependence but not regular, especially in the wavelength region $300<\lambda<600$ nm. All the samples show a characteristic peak of reflectance. High reflectance properties for ZnO is obtained as compared to the Ga-doped ZnO films especially at around 400 nm may be attributed to the increase of the refractive index of the undoped ZnO as

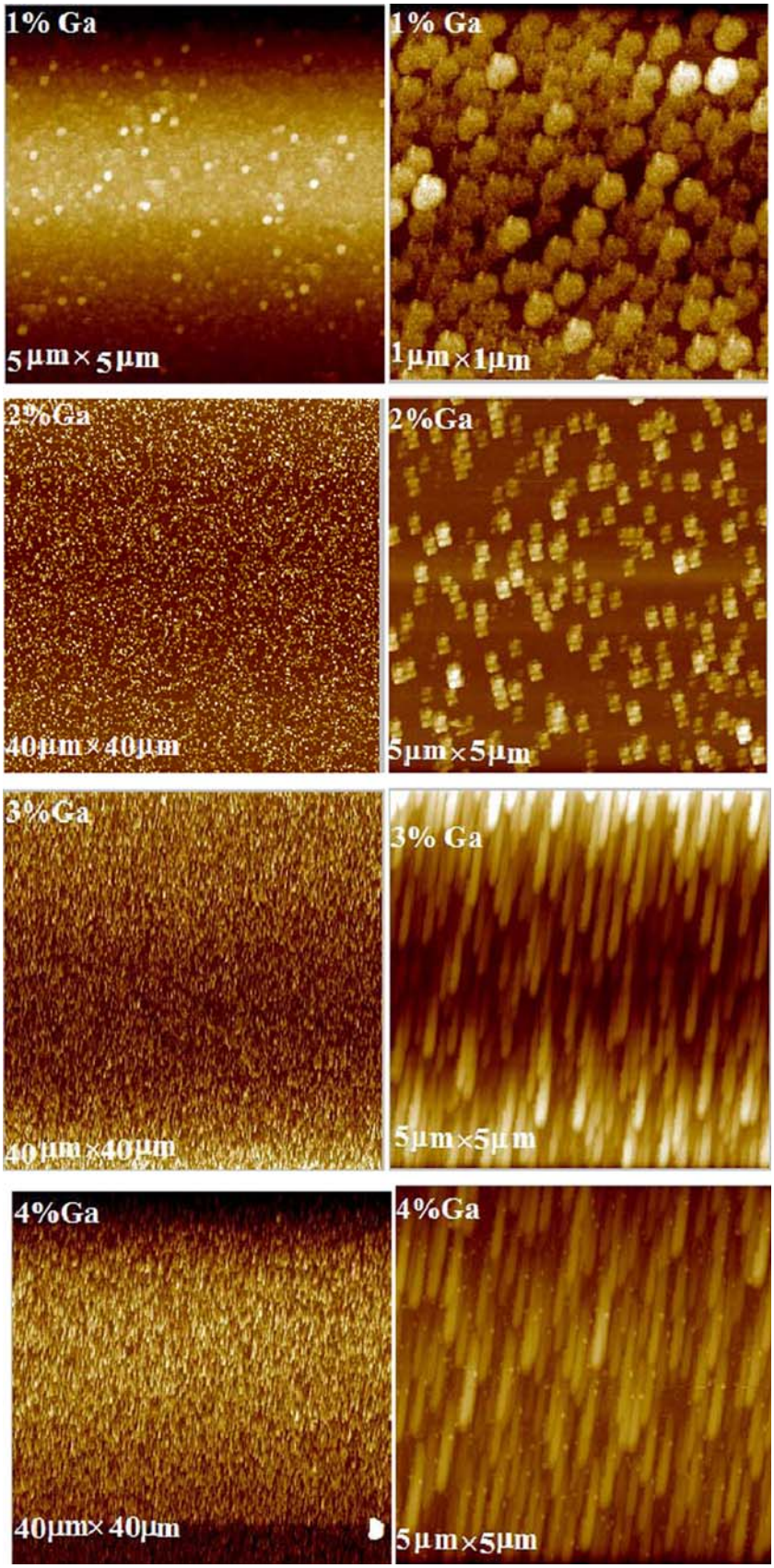

Fig. 1 AFM of ZnO and Ga-doped ZnO of 1 %,2 %,3 % and 4 % concentrations

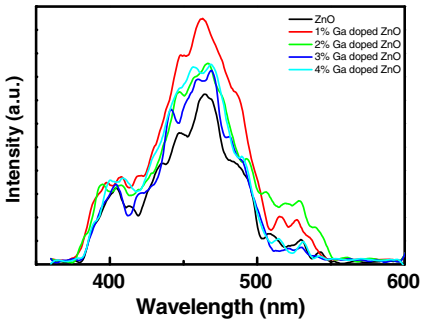

Fig. 2 Photoluminescence spectra of undoped ZnO and Ga-doped ZnO

compared to the Ga-doped ZnO. This behavior was observed by other authors [12, 14]. These effects are interesting for the fabrication of diffractive optical elements or integrated optical components [12, 29].

The oscillations in the values of T(λ) and R(λ) are a result of light interference in the considered wavelength range, one can conclude also that the light is not dispersed and this indicates that the films are homogenous [29]. The homogeneity of the films means that the thickness and/or the refractive index are uniform, also in thin transparent films. The homogeneity of the film is very important because the low homogeneity or the inhomogeneity causes a shrinking of the interference frings and a deviation of reflectance and transmittance even extrema from the reflectance and transmittance spectra of the substrate, respectively [30, 31]. Moreover, several wrong experimental conclusions could be drawn, e.g. higher extinction coefficient values than the actual ones, presence of non-existent absorption bands [30].

To obtain information about the absorption band edge of the films, the first derivative of the optical transmittance can be computed as published before by [14].

The curves of both dT/dλ and dR/dλ versus wavelength were plotted, as shown in Fig. 5(a) and (b), respectively. As seen from these figures, the maximum peak position corresponds to the absorption band edge for the ZnO and Ga-doped ZnO (1 %, 2 %, 3 % and 4 %) nanostructure films is shifted to the lower wavelengths (blue-shift). This behavior gives an evidence for the effect of the Ga dopant

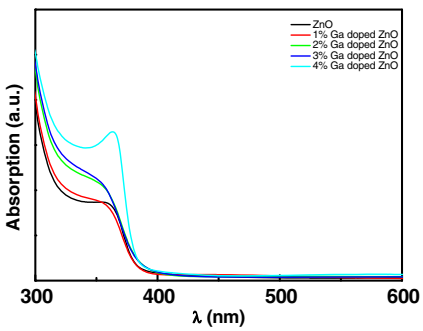

Fig. 3 Absorption spectra of undoped ZnO and Ga-doped ZnO

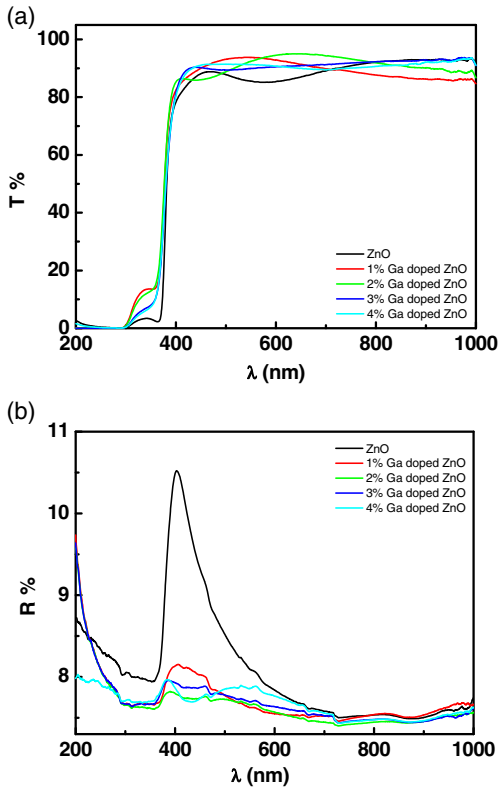

Fig. 4 (**a**) Transmission spectra of undoped ZnO and Ga-doped ZnO thin films. (**b**) Reflection spectra of undoped ZnO and Ga-doped ZnO thin films

concentrations on the ZnO and the optical band gap varies in the range 3.27–3.30 eV. It was clearly observed that the incorporation of Ga dopants increases the optical band gap value of ZnO. The incorporation of Ga dopants promoted the formation of vertically arrayed nanorods by inducing island growth in the initial stage. As we know, the optical band gap value depended upon many key parameters such as particle size, particle shape and defect concentration [32, 33]. From the results obtained and using the AFM images analysis, it is reasonable to conclude that these parameters can be influence a value of the optical band gap.

The refractive and absorption indices *n* and *k* of ZnO and Ga-doped ZnO nanostructure films were determined from the measured transmittance and reflectance at normal light incidence. The spectral dependences of both *n* (*λ*) and *k* (*λ*) are plotted in Fig. 6 (a) and (b).

The absorption index *k* is very small at longer wavelengths, showing that the prepared films are highly transparent. Evaluation of the refractive indices of optical materials is considerably important for the applications in integrated optics devices, such as switches, filters and modulation, etc., in which the refractive index is a key parameter for the device design [34].

The refractive index *n* of ZnO and Ga-doped ZnO (1 %, 2 %, 3 % and 4 %) thin film shows anomalous dispersion in

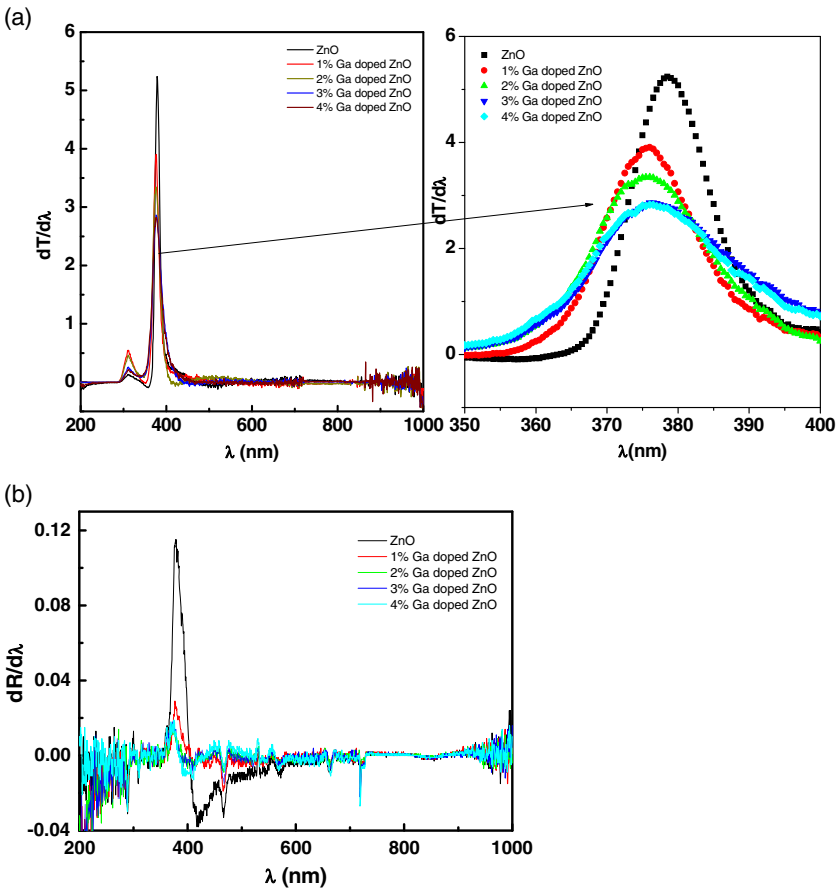

Fig. 5 (**a**) Plot of the first derivative of the transmittance, dT/dλ vs. λ of undoped ZnO and Ga-doped ZnO films. (**b**) Plot of spectral dependence of the first derivative of the reflectance, dR/dλ of undoped ZnO and Ga-doped ZnO films

the spectral range 390 <λ> 600 nm. Moreover, the films show anormal dispersion in the spectral range 600 <λ> 1000 nm. This anomalous behavior is due to the resonance effect between the incident electromagnetic radiation and the electrons polarization, which leads to the coupling of electrons in ZnO films to the oscillating electric field.

The optical absorption method was used to determine the optical band gap of the films, which is the most direct and simplest method. The fundamental absorption refers to band to band transitions and it manifests itself by a rapid rising in the absorption used to determine the optical band gap. The band-gap of the films is determined by the following relation [35]:

$$\alpha = \left(\frac{A}{h\nu}\right)\left(h\nu - E_g\right)^m, \tag{4}$$

Where, A is a constant that depends on the transition, hν is the photon energy and E_g is the optical band gap and the value of the exponent *m* depends on the nature of the optical transition type (*m* = 1/2, 1/3, 2 and 2/3 for allowed and forbidden indirect transitions, and for allowed and forbidden direct ones, respectively). An analysis of the absorption coefficient can be reasonably well fitted by Eq. (4) with *m*=1/2. This means that all the undoped and Ga doped ZnO nanostructured films have allowed direct interband transitions. Figure 7 shows the plots of $(\alpha h\nu)^2$ versus photon energy near the absorption edge of undoped and Ga doped ZnO nanostructured films. The optical band gap values of the films were determined by extrapolating the linear portion of the plot to $(\alpha h\nu)^2=0$. The obtained optical energy gap values are given in Table 1. It is clear that the obtained values of E_g are remarkably little dependence on the Ga content. The determined energy gaps for undoped and Ga doped ZnO nanostructured films thin film are in agreement with that published in the literature by other authors [36–39].

The obtained energy gap in the present work is found to be lower than that obtained for nanocrystalline Ga doped ZnO by Jung et al. [17] prepared by RF sputtering technique. But the obtained optical band gap was found to be larger than that obtained for nanocrystalline undoped and La-doped ZnO by Suwanboon and Amornpitoksuk [40]. The E_g value of ZnO altered depending on many parameters, for example, imperfection in ZnO crystal [33], particle shape [33] and particle size [41].

3.4 Optical dispersion characterization

Knowledge of the dispersion of the refractive indices of semiconductor materials is necessary for accurate modeling and design of devices [42].

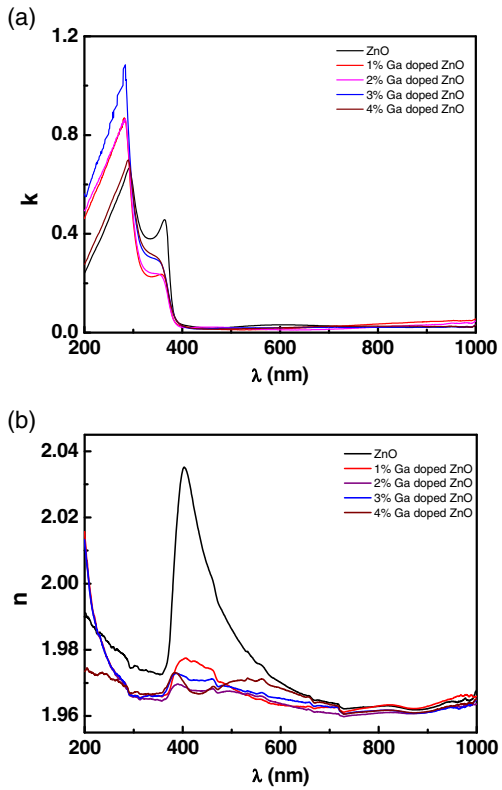

Fig. 6 (**a**) Plot of spectral dependence of absorption index of undoped ZnO and Ga-doped ZnO films. (**b**) Plot of spectral dependence of refractive index of undoped ZnO and Ga-doped ZnO films

The dispersion theory shows that in the region of low absorption, the refractive index, n, is expressed according to the effective-single oscillator model [43, 44]:

$$n^2 = 1 + \frac{E_d E_0}{E_0^2 - E^2}, \tag{5}$$

where is the photon energy, E_o is the oscillator energy and is the dispersion energy. The parameter E_d, which measures the intensity of the inter-band optical transition, does not depend significantly on the band gap. The plots of $(n^2\text{-}1)^{-1}$ versus E^2 of the ZnO and Ga-doped ZnO (1 %, 2 %, 3 % and 4 %) nanostructure films are shown in Fig. 8. As seen in Fig. 8, the refractive index is declined towards the longer wavelengths due to the influence E_o of lattice absorption. Extrapolating the linear part towards long wavelengths, the p $E_{o/}$oint of interception with the ordinate at $(h\nu)^2=0$ yields the value of the dielectric constant at higher wavelength (ε_∞). The obtained values of ε_∞ for ZnO and Ga-doped ZnO nanostructured films are given in Table 2. It is seen that the values of ε_∞ did not significantly change with Ga dopant. The obtained dispersion parameters are in agreement with that published before in the literature [13, 14, 45, 46].

Table 1 Values of energy gap for undoped and Ga-doped ZnO of 1 %, 2 %, 3%and 4 % concentrations determined from different methods

Function Ga content%	dT/dλ E_g(eV)	dR/dλ E_g(eV)	$(\alpha h\nu)^2$ E_g(eV)
0	3.277	3.280	3.255
1	3.301	3.285	3.283
2	3.307	3.290	3.295
3	3.311	3.292	3.275
4	3.313	3.293	3.285

The values of E_d and were obtained from the slope $(E_d E_o)^{-1}$ and the intersection (E_d) obtained from extrapolation of the line to zero photo energy, respectively. Figure 9 shows the variation of E_d and E_o for ZnO and Ga-doped ZnO (1 %, 2 %, 3 % and 4 %) nanostructured films. As observed, the values of E_o and E_d are found to increase with increasing Ga dopant content up to 1 % after which the values are decreased. The change in the dispersion parameters such as E_d and E_o can be attributed to the change in the polarizability, which is associated with Ga ion incorporation. The incorporation of Ga dopants promoted the formation of vertically arrayed nanorods by inducing island growth in the initial stage. As the Ga contents increased, the density of the stacking faults formed by stress relaxation process was

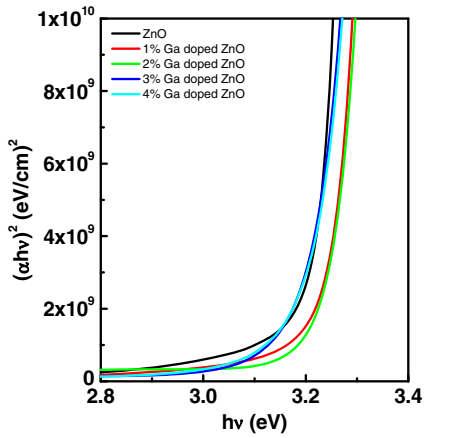

Fig. 7 Plot of photon energy dependence of $(\alpha h\nu)^2$ of undoped ZnO and Ga-doped ZnO films

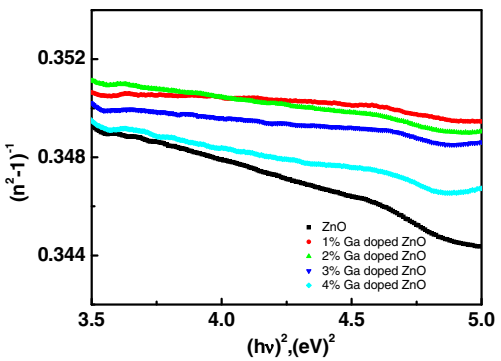

Fig. 8 Plot of $(n^2\text{-}1)^{-1}$ vs.$(h\nu)^2$ of undoped ZnO and Ni-doped ZnO films

Table 2 Dispersion Parameters of undoped and Ga-doped ZnO of 1 %, 2 %, 3 % and 4 % concentrations

Ga content%	n_{max}	ε_∞	β	ε_L	N/m*(g^{-1} cm^{-3})	f $(eV)^2$
0	2.0358	3.77	0.225	3.94	6.50×10^{46}	151.03
1	1.978	3.789	0. 285	3.87	4.78×10^{46}	132.19
2	1.969	3.79	0.275	3.8991	4.63×10^{46}	131.53
3	1.9731	3.774	0.263	3.8994	4.34×10^{46}	102.4
4	1.9739	3.735	0.203	3.939	4.15×10^{46}	63.7

greatly enhanced [47]. However, the incorporation of the Ga dopants of 3 % and 4 % forms a high density of stacking of the nanorods as obtained from AFM images.

The dispersion energy E_d, obeys the following empirical relationship [48]:

$$E_d = \beta N_c Z_a N_e \tag{6}$$

where N_c is the coordination number of the cation nearest-neighbor to the anion, Z_a is the formal chemical valency of the anion, N_e is the effective number of valence electrons per anion and β is a constant (0.37±0.04) for covalently bonded crystalline and amorphous chalcogenides and 0.26±0.04 eV for halides and most oxides that have ionic structure). Taking N_c=4, Z_a=2, N_e=8 for ZnO [48],the β values for ZnO and Ga-doped ZnO nanostructure films were determined and are given in Table 2. As observed, the obtained values of β are in agreement with that published for ZnO [45, 48] which give indication for the ionic property of the undoped and ga-doped nanostructured films.

There is an important parameter called the oscillator strength (f) as reported in [48] such that

$$f = E_0 E_d \tag{7}$$

The oscillator strength values for undoped ZnO and Ga-doped ZnO nanostructure films were determined and are given in Table 2. As observed, the obtained oscillator strength is in agreement with that published for ZnO [45, 48], but when the Ga dopant content is increased, the oscillator strength is decreased.

The obtained data of the refractive index n can be analyzed to obtain the high-frequency dielectric constant via a procedure that describes the contribution of the free carriers and the lattice vibration modes of the dispersion [49]. The relation between the optical dielectric constant, ε, and the refractive index is given by the following equation

$$\varepsilon_1 = n^2 = \varepsilon_L - D\lambda^2 \tag{8}$$

where ε_1 is the real part of the dielectric constant, ε_L is the high-frequency dielectric constant and D is a constant depending on the ratio of carrier concentration to the effective mass; $D = e^2N/4\pi^2\varepsilon_0 m^* c^2$, where e is the charge of the electron, N is the free charge carrier concentration, ε_0 is the permittivity of free space, m^* is the effective mass of the electron and c is the velocity of light. Figure 10 shows the relation between n^2 and λ for the films. It is observed that the dependence of ε_1 on λ^2 is linear at longer wavelengths. It can be shown that the refractive index has anomalous dispersion in the region of the high frequency. Aε_Ls the refractive index is increased, there is also an increased of the absorption of electromagnetic radiation associated with an increase of the frequency. Furthermore, the refractive index becomes high when the frequency of the radiation crosses with the characteristic frequency of the electron. Hence, there is no propagation of electromagnetic radiation through the ZnO films. As shown in Fig. 10, the dependence of n^2 is linear at the longer wavelengths. The value of the lattice high frequency dielectric constant ε_L is determined from the intersection of the straight line with λ^2=0. Table 2 lists the values of and the ratio N/m^* for ZnO and Ga-doped ZnO nanostructure films. The obtained values are in the order of 10^{46} $cm^{-3}.g^{-1}$. It is clear from the results that $\varepsilon_{\infty<}$ ε_L, for the

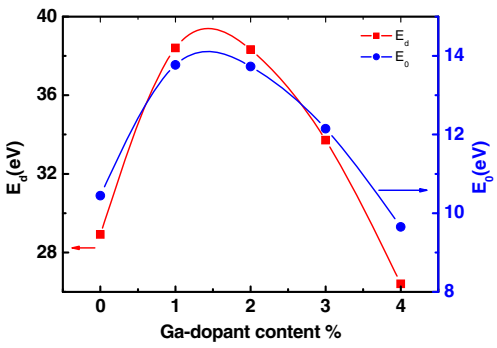

Fig. 9 Plot of E_d and E_0 vs. Ga-dopant content %

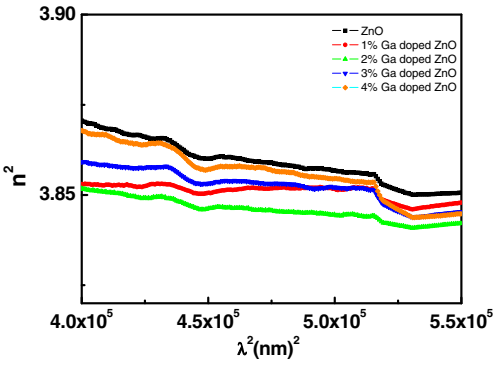

Fig. 10 Plot of n^2 vs. λ^2 of undoped ZnO and Ga-doped ZnO films.

all films which can be attributed to the contribution of the free charge carrier. In general, it can be concluded that both the high frequency dielectric constant and the ratio N/m* are related to the internal microstructure [50].

3.5 Dielectric characterization

The fundamental electron excitation spectrum of the films was described by means of the frequency dependence of the complex dielectric constant [51]. The complex refractive index $\hat{n} = n + ik$ and dielectric function $\hat{\varepsilon} = \varepsilon_1 + i\varepsilon_2$ characterize the optical properties of any solid material. The real and imaginary parts of complex dielectric constant are expressed by the following relation [52]:

$$\varepsilon_1(\omega) = n^2(\omega) - k^2(\omega), \tag{9a}$$

$$\varepsilon_2(\omega) = 2n(\omega)k(\omega), \tag{9b}$$

where ε_1 and ε_2 are the real and imaginary parts of the dielectric constant, respectively. The dependences of ε_1 and ε_2 on the photon energy are shown in Fig. 11 (a) and (b) for ZnO and Ga-doped ZnO nanostructure films. The real and imaginary parts follow different patterns. The variation of the dielectric constant with photon energy indicates that some interactions between photons and electrons in the films are produced in this energy range. These interactions are observed on the shapes of the real and imaginary parts of the dielectric constant and they cause formation of peaks in the dielectric spectra which depends on the material type [52].

The real and imaginary parts of the dielectric constant ε_1 and ε_2 can be used to calculate the spectral behavior of the optical conductivity according to the following relations [53]:

$$\sigma^*(\omega) = \sigma_1(\omega) + i\sigma_2(\omega) \tag{10}$$

where

$$\sigma_1(\omega) = \omega\varepsilon_0\varepsilon_2 \tag{10a}$$

$$\sigma_2(\omega) = \omega\varepsilon_0\varepsilon_1 \tag{10b}$$

Where $\sigma_1(\omega)$ and $\sigma_2(\omega)$ are the real and imaginary parts of the optical conductivity, respectively, ε_0 is the permittivity of the free space. The optical conductivities $\sigma_1(\omega)$ and $\sigma_2(\omega)$ can be used to detect any further allowed interband optical transitions. The dependence of the real and

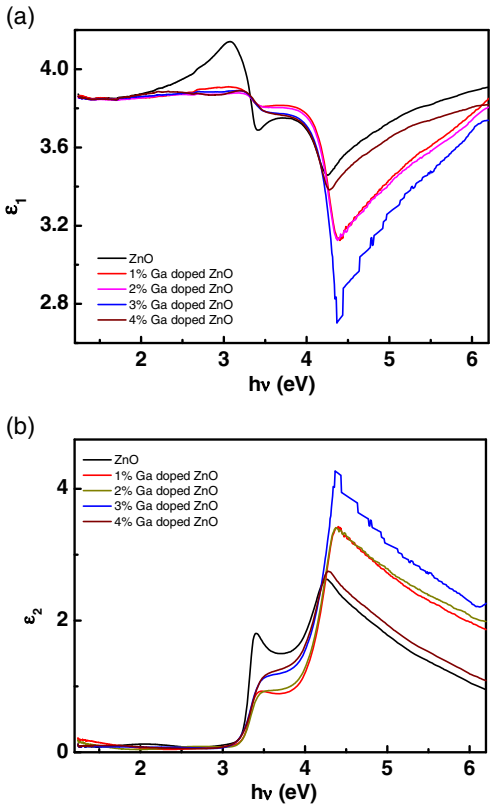

Fig. 11 (**a**) Plot of photon energy dependence of real dielectric constant of undoped ZnO and Ga-doped ZnO films. (**b**) Plot of photon energy dependence of imaginary dielectric constant of undoped ZnO and Ga-doped ZnO films

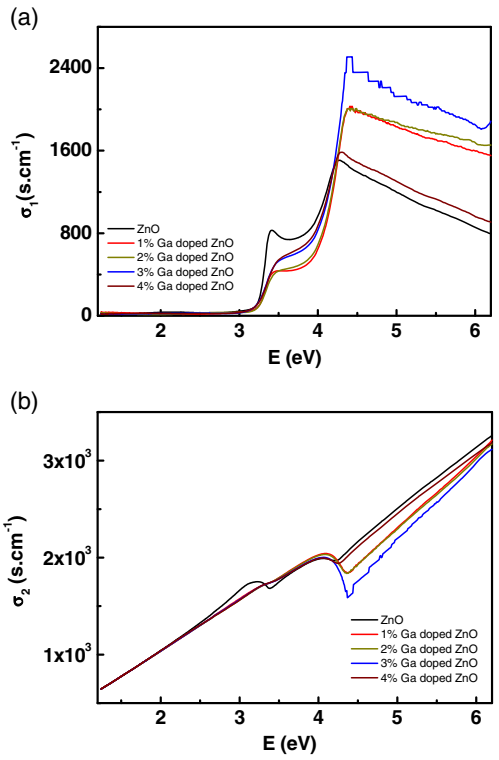

Fig. 12 (**a**) Plot of photon energy dependence of real optical conductivity of undoped ZnO and Ga-doped ZnO films. (**b**) Plot of photon energy dependence of imaginary optical conductivity of undoped ZnO and Ga-doped ZnO films

imaginary parts of the optical conductivity on the wavelength is shown in Fig. 12(a) and (b). It can be seen that the real and imaginary optical conductivity values are little affected by Ga doping concentration at lower photon energy up to about 3 eV, after which the undoped ZnO has a high optical conductivity in the photon energy region 3.2–4 eV for the real and in the range 2.5–3.2 eV for the imaginary optical conductivity. At the higher photon energy range (larger than 4 eV up to 6 eV), the undoped ZnO has the lower values of real optical conductivity and higher imaginary optical conductivity but the Ga-doped ZnO of 3 % concentration has the higher values of real optical conductivity and lower imaginary optical conductivity. The lower value of the real optical conductivity of undoped ZnO may be attributed to the high reflectance properties of ZnO as compared to the Ga-doped ZnO films [12, 14].

4 Conclusions

Nanostructure films of undoped ZnO and Ga-doped ZnO (1 %, 2 %, 3 % and 4 %) were grown by sol–gel spin coating process. Nanorods were observed for Ga-doped ZnO films with concentrations of 3 % and 4 % as obtained from AFM images. Photoluminescence (PL) spectra of undoped ZnO and Ga doped showed a strong emission band at about 465 nm. The optical constants of the undoped and Ga doped ZnO films of different concentrations were characterized using spectrophotometric measurements. It was found that the absorption spectra near the band edge could be well fitted using the direct transitions and little effect of Ga concentration was observed on the obtained energy gap of the films. On the other hand, it was found that the refractive index of the Ga deposited film is affected with doping concentration of Ga. In addition, Ga-doping concentration affects the values of the calculated dispersion parameters such as oscillator energy, dispersion energy, oscillator strength and dielectric constants. Moreover, a higher real and imaginary optical conductivity were obtained for the Ga-doped ZnO of 3 % concentration and undoped ZnO, respectively.

Acknowledgement This research was supported by the Korea Research Foundation Grant through the Human Resource Training Project for Regional Innovation funded by 2010 the Korean Government which was conducted by the Ministry of Education, Science and Technology.

References

1. V.I. Kushnirenko, I.V. Markevich, T.V. Zashivailo, J. Lumin. **132**, 1953 (2012)
2. K. Wolff, U. Hilleringmann, Solid-State Electron. **67**, 11 (2012)
3. A. Crossay, S. Buecheler, L. Kranz, J. Perrenoud, C.M. Fella, Y.E. Romanyuk, A.N. Tiwari, Sol. Energy Mater. Sol. Cells **101**, 283 (2012)
4. C. Chen, P. Yang, Y. Shen, S. Ma, S. Shiu, S. Hung, S. Lin, C. Lin, Sol. Energy Mater. Sol. Cells **101**, 180 (2012)
5. H.W. Kim, H.G. Na, J.C. Yang, C. Lee, Chem. Eng. J. **171**, 1439 (2011)
6. Y. Li, K. Li, C. Wang, C. Kuo, L. Chen, Sensor Actuat. B-Chem. **161**, 734 (2012)
7. P. Li, S. Wang, J. Li, Y. Wei, J. Lumin. **132**, 220 (2012)
8. S. Vijayalakshmi, S. Venkataraj, R. Jayavel, J. Phys. D: Appl. Phys. **41**, 245403 (2008)
9. F.K. Shan, G.X. Liu, W.J. Lee, B.C. Shin, J. Cryst. Growth **291**, 328 (2006)
10. Y. Caglar, S. Ilican, M. Caglar, F. Yakuphanoglu, Spectrochim. Acta A **67**, 1113 (2007)
11. S. Ilican, Y. Caglar, M. Caglar, F. Yakuphanoglu, J. Cui, Physica E **41**, 96 (2008)
12. F. Yakuphanoglu, S. Ilican, M. Caglar, Y. Caglar, Superlattice Microst. **47**, 732 (2010)
13. A.A.M. Farag, M. Cavaş, F. Yakuphanoglu, F.M. Amanullah, J. Alloys Compd. **509**, 7900 (2011)
14. M. Caglar, F. Yakuphanoglu, Appl. Surf. Sci. **258**, 3039 (2012)
15. P.K. Nayak, J. Yang, J. Kim, S. Chung, J. Jeong, C. Lee, Y. Hong, J. Phys. D: Appl. Phys. **42**, 035102 (2009)
16. K. Yoshino, T. Hata, T. Kakeno, H. Komaki, M. Yoneta, Y. Akaki, T. Ikari, Phys. Stat. Sol. (c) **0**, 626 (2003)
17. K. Jung, W. Choi, S. Yoon, H.J. Kim, J. Choi, Ceram. Int. **38S**, S605 (2012)
18. M.M. El-Nahass, A.A.M. Farag, A.A. Atta, Synth. Met. **159**, 589 (2009)
19. P.P. Banerjee, Proc. IEEE **73**, 1859 (2005)
20. Y.Y. Kim, B.H. Kong, H.K. Cho, J. Cryst. Growth **330**, 17 (2011)
21. S. Ameen, M. Shaheer Akhtar, H. Seo, Y.S. Kima, H.S. Shin, Chem. Eng. J. **187**, 351 (2012)
22. X. Liu, X. Wu, H. Cao, R.P.H. Chang, J. Appl. Physics **95**, 3141 (2004)
23. R. Elilarassi, G. Chandrasekaran, Mater. Sci. Semicond. Process. **14**, 179 (2011)
24. M.K. Patra, K. Manzoor, M. Manoth, S.R. Vadera, N. Kumar, J. Phys. Chem. Solids **70**, 659 (2009)
25. A. Wang, B. Zhang, X. Wang, N. Yao, Z. Gao, Y. Ma, L. Zhang, H. Ma, J. Phys. D: Appl. Phys. **41**, 215308 (2008)
26. B. Kumar, H. Gong, S. Vicknesh, S.J. Chua, S. Tripathy, Appl. Phys. Lett. **89**, 071922 (2006)
27. R.S. Yadav, M. Priya, C.P. Avinash, Ultrason Sonochem. **15**, 863 (2008)
28. X.L. Wu, G.G. Siu, C.L. Fu, H.C. Ong, Appl. Phys. Lett. **78**, 2285 (2001)
29. M.M. El-Nahass, H.M. Zeyada, A.A. Hendi, Opt. Mater. **25**, 43 (2004)
30. L. De Caro, M.C. Ferrara, Thin Solid Films **342**, 153 (1999)
31. K. Bah, A. Czapla, T. Pisarkiewicz, Thin Solid Films **232**, 18 (1993)
32. S. Suwanboon, P. Amornpitoksuk, Procedia Eng. **32**, 821 (2012)
33. S. Suwanboon, P. Amornpitoksuk, P. Bangrak, A. Sukolrat, N. Muensit, J. Ceram Process Res. **11**, 547 (2010)
34. D.A. Minkov, J. Phys. D: Appl. Phys. **22**, 1157 (1989)
35. S.K. Gagandeep, B.S. Lark, H.S. Sahota, Nucl. Sci. Eng. **134**, 208 (2000)
36. R. Rusdi, A. Abd Rahman, N. Sabirin Mohamed, N. Kamarudin, N. Kamarulzaman, Powder Technol. **210**, 18 (2011)
37. F.K. Shan, Y.S. Yu, J. Eur. Ceram. Soc. **24**, 1869 (2004)
38. Y. Wu, H. Chen, J. Magn. Magn. Mater. **324**, 2153 (2012)
39. F. Li, C. Liu, Z. Ma, L. Zhao, Opt. Mater. **34**, 1062 (2012)
40. S. Suwanboon, P. Amornpitoksuk, Ceram. Int. **37**, 3515 (2011)

41. S. Suwanboon, P. Amornpitoksuk, S. Muensit, J. Ceram. Process. Res. **11**, 419 (2010)
42. C. Jagadish, S.J. Pearton, *Zinc Oxide Bulk, Thin Films Nanostructures: Processing, Properties, and Applications* (Elsevier Ltd., Hong Kong, 2006)
43. S.H. Wemple, M. Didomenico, J. Phys. Rev. B **3**, 1338 (1971)
44. S.H. Wemple, M. Didomenico, J. Phys. Rev. B **7**, 3767 (1973)
45. Z. Serbetc, H.M. El-Nasser, F. Yakuphanoglu, Spectrochim. Acta A **86**, 405 (2012)
46. S. Ilican, Y. Caglar, M. Caglar, F. Yakuphanoglu, Appl. Surf. Sci. **255**, 2353 (2008)
47. Y.Y. Kim, B.H. Kong, H.K. Cho, J. Crys. Growth **330**, 17 (2011)
48. S.H. Wemple, M. DiDomenico, J. Phys. Rev. Lett. **23**, 1156 (1969)
49. G.A. Kumar, J. Thomas, N. George, B.A. Kumar, P. Radhakrishnan, V.P.N. Nampoori, C.P.G. Vallabhan, J. Phys. Chem. Glasses **41**, 89 (2000)
50. G.A. Mohamed, E. Mohamed, A. Abu El El-Fadl, Physica B **308**, 949 (2001)
51. T.S. Moss, G.J. Burrell, B. Ellis, *Semiconductor Opto-Electronics* (Wiley, New York, 1973)
52. A.A.M. Farag, I.S. Yahia, Opt. Commun. **283**, 4310 (2010)
53. F. Yakuphanoglu, M. Sekerci, O.F. Ozturk, Opt. Commun. **239**, 275 (2004)